Click Here for Full Article

Reservoir infill by hyperpycnal deltas over bedrock

Steven Y. J. Lai[1] and H. Capart[1]

Received 29 December 2008; accepted 23 February 2009; published 21 April 2009.

[1] We propose a simple morphodynamic theory of reservoir deltas prograding over bedrock under the influence of turbid underflows. The theory models the geomorphic actions of fluvial and hyperpycnal flows as diffusion processes, and treats bedrock-alluvial and river-lake transitions as moving internal boundaries. It yields self-similar analytical solutions for the co-evolving river and lake bed profiles, under different slope and influx conditions. These include a special case in which delta deposits are swept underwater to prograde into a subaqueous turbid pool. The theoretical predictions are in good agreement with microscale experiments, and should help interpret and anticipate longitudinal sedimentation patterns in mountain reservoirs.
Citation: Lai, S. Y. J., and H. Capart (2009), Reservoir infill by hyperpycnal deltas over bedrock, *Geophys. Res. Lett.*, *36*, L08402, doi:10.1029/2008GL037139.

1. Introduction

[2] Severe rates of sediment infill affect many reservoirs in the tectonically active mountains of Taiwan and Japan [*Dadson et al.*, 2003; *Kashiwai*, 2005]. In Central Taiwan upstream of Wushe Dam, for instance, deltaic deposits prograded a distance of about 1 km into the reservoir in the last two years alone (Figures 1a and 1b), while the river bed aggraded up to two stories high 5 km upstream. To forecast reservoir capacity losses and upstream river changes in such valleys, a model of the spatial distribution of sediment deposition is required. Currently, however, no interpretative or predictive model is available that embraces the variety of depositional patterns observed in practice [*Morris and Fan*, 1997]. Here we propose a simple theory of river and lake bed evolution, applicable to deltas over bedrock subject to fluvial and hyperpycnal influences. The theory extends the approach of *Lai and Capart* [2007], and draws from earlier work on fluvial, lacustrine and submarine diffusion [*Begin et al.*, 1981; *Kenyon and Turcotte*, 1985; *Jordan and Flemings*, 1991], as well as recent work on moving boundary problems [*Voller et al.*, 2004; *Capart et al.*, 2007]. Below we describe the theory before testing it using experiments.

2. Theory

[3] Motivated by the typical characteristics of mountain reservoirs in Taiwan and Japan (Figure 1), we consider a long, narrow lake created by damming a valley with bedrock sides and floor. Neglecting width variations, we examine the longitudinal profile morphodynamics of the river and lake beds. Alimented by the products of landsliding [*Imaizumi and Sidle*, 2007], supply-limited sediment transport drapes deltaic deposits over the bedrock floor both upstream and downstream of the river-lake transition (Figure 1c). Upstream, aggradation of the delta topset raises the river bed, driving the headward migration of a transition between exposed bedrock and alluvial cover [*Muto*, 2001]. Downstream, a delta foreset progrades into the reservoir. Sediment transport along the foreset bed is driven by plunging underflows if the density of the turbid river exceeds that of the lake (hyperpycnal case), or by gravitational avalanching otherwise (homo- or hypopycnal case) [*Lai and Capart*, 2007]. In the hyperpycnal case, turbid currents flow along the lake bottom before ponding at the deep end of the reservoir [*Toniolo et al.*, 2007], where they may be vented using bottom outlets [*Fan*, 1986]. For simplicity, we assume that spilling and venting keep the reservoir waterline and the internal density interface of the subaqueous turbid pool at constant levels. We focus on the deposition of relatively coarse sediment along the delta topset and foreset, and neglect bed elevation changes due to very fine sediment settling out of the fluvial and hyperpycnal flows. Bottom set beds are thus excluded from consideration.

[4] We assume that the bedrock river has initial profile $z_0(x) = -S_0 x$, where $S_0 = \tan\theta$ is the bedrock inclination and spatial coordinate x is measured in the direction of the valley axis. A steady river flow rate Q discharges into the reservoir maintained at constant level $z = 0$. Starting from bare bedrock, at time $t = 0$, the upstream reach of the river is supplied with sediment at steady volumetric rate I. As this flux is lower than the transport capacity of the bedrock river (supply-limited conditions), sediment will not deposit before reaching the aggrading delta. The deltaic profile evolution is subject to the Exner equation

$$\frac{\partial z}{\partial t} + \frac{\partial j}{\partial x} = 0 \tag{1}$$

where $z(x, t)$ is the bed profile elevation above base level and $j(x, t)$ is the sediment transport rate, taken as a volumetric flux of bed material (sediment + pore space) per unit width. Bedrock and angle-of-stability constraints require that

$$z(x,t) \geq z_0(x), \qquad |\partial z/\partial x| \leq R, \tag{2}$$

where $R = \tan\varphi$ is the slope beyond which avalanching occurs. Except where avalanching takes place, we assume that the sediment transport rate j is governed by the modified diffusive relation

$$j(x,t) = D(S - S_{\min}), \tag{3}$$

where D is the diffusivity, $S = -\partial z/\partial x$ is the local bed inclination, $S_{\min}$ is a minimum inclination required for

[1]Department of Civil Engineering and Hydrotech Research Institute, National Taiwan University, Taipei, Taiwan.

Copyright 2009 by the American Geophysical Union.
0094-8276/09/2008GL037139$05.00

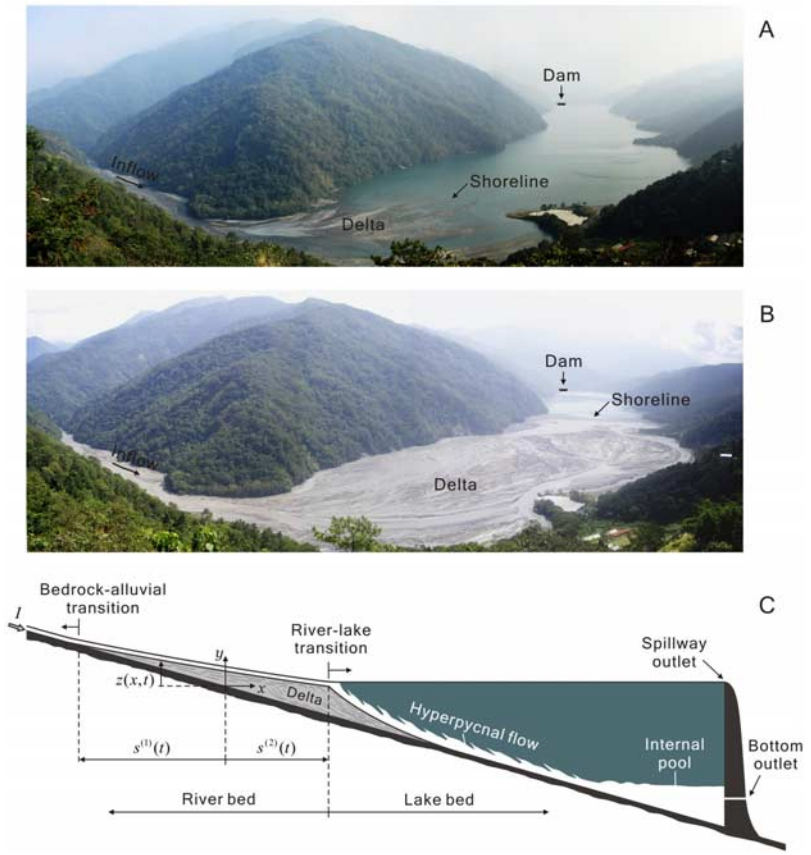

Figure 1. Deltas prograding over bedrock into narrow reservoirs. Wanda Reservoir, central Taiwan, upstream of Wushe Dam (a) on October 21, 2006, and (b) on October 5, 2008 (photos by H. Capart). (c) Schematic long profile of a hyperpycnal delta in a generic mountain reservoir [adapted from *Morris and Fan*, 1997; *Lai and Capart*, 2007].

sediment transport, and it is implied that $S > S_{\min}$. Alternatively, this relation can be interpreted as a two-term approximation to a more complicated empirical or predictive sediment transport law [*Hsu and Capart*, 2008]. We found in earlier work [*Lai and Capart*, 2007] that equation (3) can be applied to both the topset and foreset of hyperpycnal deltas provided that different values D_1, D_2, for the diffusivity, and $S_{\min,1}$, $S_{\min,2}$ for the minimum inclination are considered for fluvial and hyperpycnal transport.

[5] For deltas over bedrock (Figure 1c), let $s^{(1)}(t)$, $s^{(2)}(t)$ denote the positions of the bedrock-alluvial and river-lake (or topset-foreset) transitions. Upon substituting equation (3) in equation (1), we obtain the two diffusion equations

$$\frac{\partial z_1}{\partial t} - D_1 \frac{\partial^2 z_1}{\partial x^2} = 0, \qquad s^{(1)}(t) < x < s^{(2)}(t), \tag{4}$$

$$\frac{\partial z_2}{\partial t} - D_2 \frac{\partial^2 z_2}{\partial x^2} = 0, \qquad s^{(2)}(t) < x, \tag{5}$$

where D_1 and D_2 are the subaerial and subaqueous diffusivities ($D_1 > D_2$), and $z_1(x, t)$ and $z_2(x, t)$ are the topset and foreset profiles (Figure 1c). Like the single moving boundaries treated by *Voller et al.* [2004] and *Capart et al.* [2007], the two moving boundaries $s^{(1)}(t)$, $s^{(2)}(t)$ migrate according to

$$s^{(\beta)}(t) = \lambda^{(\beta)} \sqrt{D_1 t}, \qquad \beta = 1, 2, \tag{6}$$

where $\lambda^{(1)}$ and $\lambda^{(2)}$ are dimensionless constants governing the time-evolving positions of the delta boundaries. Analytical solutions for the bed profiles $z_\alpha(x, t)$, $\alpha = 1, 2$, then take the self-similar form [for a derivation, see *Capart et al.*, 2007]

$$\frac{z_\alpha}{\sqrt{D_\alpha t}} = -A_\alpha \frac{x}{\sqrt{D_\alpha t}} + B_\alpha \,\mathrm{ierfc}\left(\frac{x}{2\sqrt{D_\alpha t}}\right) \tag{7}$$

where the special function ierfc is the first integral of the complementary error function. The coefficients A_1, B_1, for the topset, A_2, B_2, for the foreset, and $\lambda^{(1)}$, $\lambda^{(2)}$, for the moving boundaries, are obtained from the internal and external boundary conditions. These include, at the bedrock-alluvial and river-lake transitions, the prescribed elevations

$$\begin{aligned} z_1(s^{(1)}(t), t) &= -S_0 s^{(1)}(t), \\ z_1(s^{(2)}(t), t) &= z_2(s^{(2)}(t), t) = 0, \end{aligned} \tag{8}$$

as well as continuity of the sediment fluxes

$$\begin{aligned} j_1(s^{(1)}(t), t) &= I, \\ j_1(s^{(2)}(t), t) &= j_2(s^{(2)}(t), t). \end{aligned} \tag{9}$$

where $j_\alpha = D_\alpha(-\partial z_\alpha/\partial x - S_{\min,\alpha})$, $\alpha = 1, 2$. Two boundary conditions must be applied at each transition because their migration histories are part of the problem to be solved.

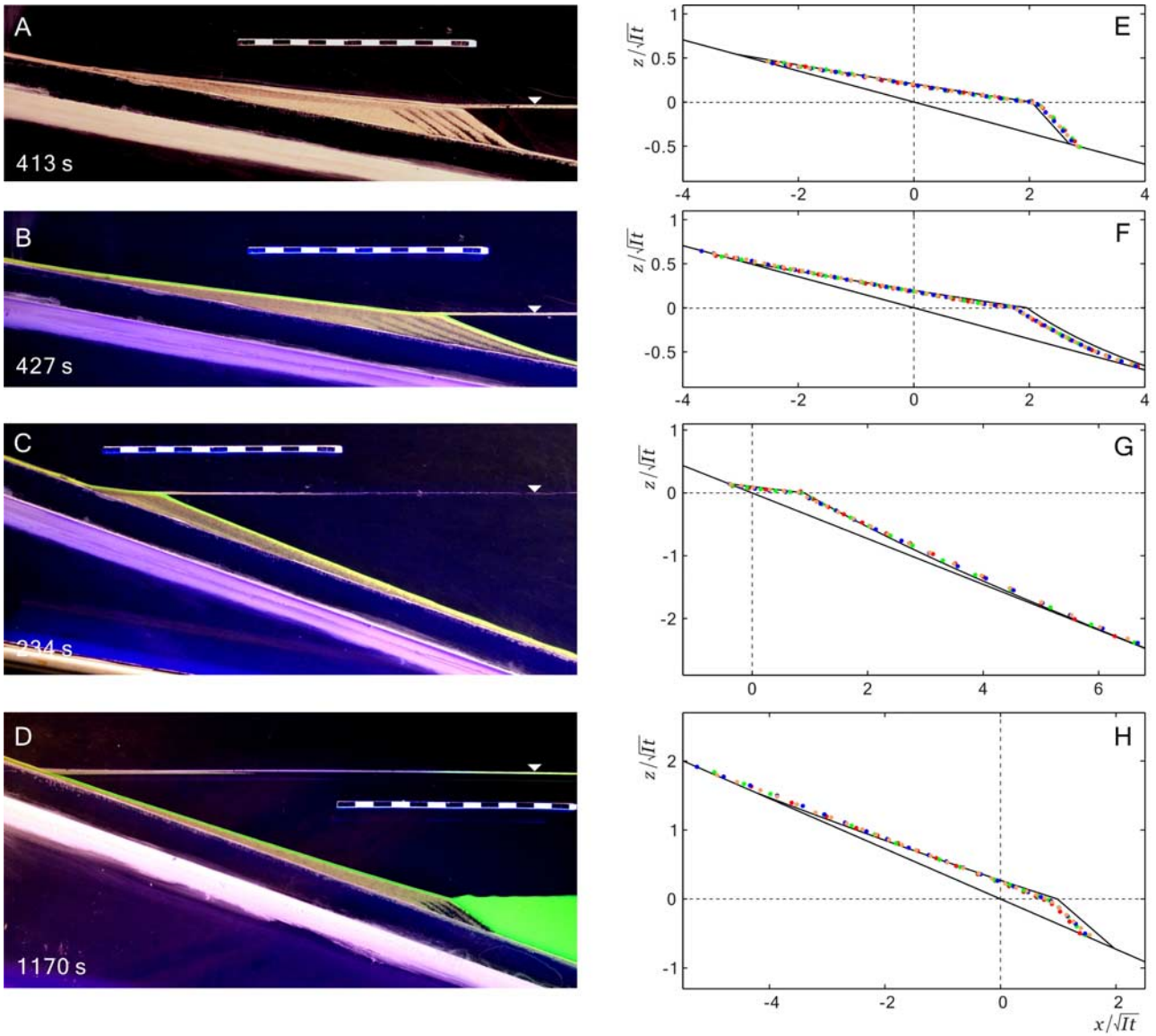

Figure 2. Left: experimental deltas over bedrock: (a) homopycnal delta (sediment influx $I = 5.7$ mm^2 s^{-1}, bedrock inclination $\theta = 10°$); (b) hyperpycnal delta ($I = 5.2$ mm^2 s^{-1}, $\theta = 10°$); (c) hyperpycnal delta over steeper bedrock slope ($I = 5.2$ mm^2 s^{-1}, $\theta = 20°$); (d) hyperpycnal delta supplied with lower rate of sediment influx ($I = 0.94$ mm^2 s^{-1}, $\theta = 20°$). Right: comparison of measured (dots) and theoretical profiles (lines). Data points colored red, green, blue, and orange denote delta profiles measured at evenly spaced time t_1 to t_4. Normalized coordinates are used to demonstrate self-similarity.

[6] Two additional cases can be addressed by slightly modifying the above model. For homopycnal conditions, the subaqueous diffusivity D_2 becomes equal to zero, and avalanching takes over instead of underflow-driven sediment transport along the delta front. Equations and boundary conditions for the river bed are the same as before, save for the sediment flux condition at the shoreline which becomes [*Voller et al.*, 2004; *Capart et al.*, 2007]

$$j_1(s^{(2)}(t), t) = \frac{RS_0(\lambda^{(2)})^2}{2(R - S_0)}. \tag{10}$$

Finally, if the sediment influx I is weak compared to the transport capacity of the underflow, $I < D_2\ (S_0 - S_{\min,2})$, deltaic deposits can be completely swept into the lake. The sediment load then bypasses the river-lake transition to form a subaqueous delta prograding into the turbid pool. Hyperpycnal flow drives transport along the topset, and the base level ($z = 0$) must be switched from the waterline to the internal density interface, under which avalanching occurs.

3. Experiments

[7] To test the ability of the theory to model different types of deltas over bedrock, we use microscale experiments. These are performed at such small scales that flows are laminar instead of turbulent, yet they can still be scaled up to field dimensions under certain conditions [*Malverti et al.*, 2008]. Experiments are conducted in a narrow flume

(length = 1 m; width = 1 cm), constructed with transparent parallel walls and a rough, rigid floor. Downstream, the flume is fitted with weirs to control the lake waterline and subaqueous density interface. Upstream, the river discharge is supplied by a constant head tank, and the sediment influx by a conveyor belt. For the river discharge, either freshwater ($\rho = 1.0$ g ml^{-1}) or brine ($\rho = 1.2$ g ml^{-1}) are used to obtain homopycnal or hyperpycnal inflows into the freshwater lake. For the sediment, fine sand of median diameter d_{50} = 0.17 mm, coefficient of uniformity $d_{60}/d_{10} = 2.3$, and angle of repose $\varphi = 36°$ is chosen. Green fluorescent dye is added to the brine to visualize underflows, and black ash is sprinkled at repeated intervals to visualize the stratigraphy of the deposits. Time-lapse photography is used to monitor the evolution of the river and lake beds, with photos acquired at intervals of 5 sec. Bed elevation measurements are obtained by digitizing profiles from the timelapse photographs and translating them to metric coordinates using a calibrated transform.

[8] We present on Figure 2 four experiments designed to document the effects of inflow density (homopycnal versus hyperpycnal), inclination (moderate to steep), and sediment supply (high to low) on the morphology of deltas over bedrock. To gauge the influence of inflow density, experiments A and B (Figures 2a and 2b) show deltaic morphologies resulting from homopycnal and hyperpycnal river inflows, respectively, over bedrock floors of moderate inclination ($\theta = 10°$). Microscale experiments with homopycnal deltas over bedrock were reported earlier [*Muto*, 2001], hence experiment A serves as a baseline case. To examine the effect of inclination, experiment C is conducted under the same hyperpycnal conditions as experiment B, with the steepness of the bedrock floor increased twofold to $\theta = 20°$. Experiment D shows what happens under the same conditions when the sediment supply is decreased by a factor of 5, and the hyperpycnal current ponds into a subaqueous pool at the downstream end of the flume. To facilitate comparison, all tests are performed under the same river discharge, held steady at volumetric flow rate per unit width $Q = 80.6$ mm^2 s^{-1}. For small scale experiments, transport relations are expected to take the following power law form [see, e.g., *Swenson and Muto*, 2007; *Hsu and Capart*, 2008]

$$j(x,t) = aQS^b, \tag{11}$$

instead of the simpler equation (3), where a and b are dimensionless empirical coefficients. To translate from equation (11) to equation (3), we use a two term Taylor expansion around a reference slope S_{ref}. We set $S_{\mathrm{ref}} = S_{\mathrm{eq}}$ for fluvial transport and $S_{\mathrm{ref}} = \frac{1}{2}(S_0 + S_{\mathrm{eq}})$ for hyperpycnal transport, where $S_{\mathrm{eq}} = (I/(aQ))^{1/b}$ is the slope that equilibrates the sediment influx I. Different values of coefficient a apply to fluvial and hyperpycnal transport, but a common exponent b is used.

4. Experimental Results

[9] Depicted by the photographs of Figure 2 (left column) are the mature deltaic deposits formed at late stages of the four experiments, when the shallow fluvial and hyperpycnal flows (from left to right) are still active. Experiment A (Figure 2a), performed under homopycnal conditions, leads to a classical Gilbert delta, with a topset of mild inclination, a steep foreset inclined at the angle of repose ($\varphi = 36°$), and sharp slope breaks at the shoreline and foreset toe. Experiment B (Figure 2b), by contrast, shows the influence of hyperpycnal conditions (ratio of river density to lake density = 1.2). Under the influence of the gravity underflow (thin green layer), the foreset becomes more elongated, reduces its maximum inclination (to well below the angle of repose), and adopts a concave upwards curvature allowing the foreset toe to connect smoothly with the lake bottom. Unlike the subaqueous foresets, the subaerial topsets of experiments A and B are similar to each other in shape and inclination. In both cases, the topset terminates upstream at a well-defined transition between exposed bedrock and alluvial cover, which migrates headward as the delta grows.

[10] Experiment C (Figure 2c) provides further information about the response of the bedrock-alluvial transition. For this steeper inclination ($\theta = 20°$), the hyperpycnal flow drives a greater proportion of the river sediment load into the lake. The delta foreset becomes highly elongated, leaving only a short topset between the bedrock-alluvial transition and the shoreline. Experiment D (Figure 2d), finally, confirms that it is possible for hyperpycnal flows over bedrock to drive the entire river sediment load into the lake, provided that the sediment supply is sufficiently low. Upon reducing the sediment supply by a factor of 5 (compared to experiment C), the hyperpycnal underflow is able to drive the entire river sediment flux through the shoreline, making the subaerial delta disappear. A subaqueous delta forms instead, prograding into the turbid pool. Despite their different environments, the subaqueous delta of experiment D is quite similar in morphology to the subaerial delta of experiment A. Both feature short, straight foresets inclined at the angle of repose, and long topsets of mild concave upwards curvature. Where they differ is in their topset inclination, much steeper in the subaqueous case D than in the subaerial case A, and in their speed of accumulation, much slower in case D due to the reduced influx. Cases C and D underscore that, over the same bedrock inclination, it is possible for lake deposits to exhibit very different depositional patterns. Dependent on the sediment influx (strong versus weak), downstream (case C) or upstream tapering (case D) of the underwater deposits is observed, flipping the direction in which deposits become gradually thinner.

5. Comparison and Discussion

[11] Measured river and lake bed profiles are plotted in Figure 2 (right column). A consequence of the theory is that, for each experiment, delta profiles acquired at different times should collapse together when plotted in normalized coordinates $x/\sqrt{It}$, $z/\sqrt{It}$. This geometrical self-similarity is verified to a very good approximation by the experimental data (dots obtained at four different times t_1 to t_4 collapse together). The delta morphology is thus independent of the time of observation, and delta growth produces an internal stratigraphy composed of nested profiles representing homothetic replicas of each other. This explains, on Figures 2a–2d, the self-similar stacking of trapped ash layers in the experimental deposits. Because of self-similarity, moreover, the sediment flux j at any location

s can be estimated from each measured profile $z(x, t)$ using the integral formula

$$j(s,t) = I + \frac{(z(s,t) - z_0(s))s}{2t} - \frac{1}{t}\int_{-\infty}^{s} (z(x,t) - z_0(x))dx, \quad (12)$$

and the bed inclination S at the same location can be estimated by differencing. Using this inversion formula, one could in principle reconstruct sediment transport rates from surveyed delta profiles, or from past delta profiles preserved in the stratigraphic record. Here we apply the formula to our experimental profiles and use the resulting empirical relationship $j(S)$ to calibrate the transport coefficients a and b in equation (11). The obtained values are $a = 130$ for fluvial transport, $a = 0.65$ for hyperpycnal transport, and $b = 3.5$ for the exponent. Using the same calibrated values for all cases, the theoretical profiles plotted in Figures 2e–2h are found to be in close agreement with the measured data. The bed shapes and elevations are well predicted, with only slight errors in phase for the positions of the delta fronts. Most important, the theory is able to reproduce the wide behavioral range of the experimental deltas. This range includes the production of straight and curved foresets (A versus B), contrasted ratios of foreset to topset length (B versus C), and the formation of underwater deposits of opposite tapers (C versus D). To check that such agreement is not restricted to laminar microscale experiments, we also tested the theory against turbulent Froude scale experiments by *Armanini and Larcher* [2001], for case A, and *Yu et al.* [2000], for case C. Although different values are obtained for the transport coefficients, profile results are in good agreement and suggest that the theoretical framework itself is scale-independent. The theory may therefore help make sense of the very different depositional patterns that have been documented in mountain reservoirs. In Taiwan, a Gilbert-type delta similar to case A has led to the recent infill of the small Ronghua reservoir, upstream of the large Shimen reservoir [*Capart et al.*, 2007]. In the Ronghua case, river inflow is highly turbid during flood [*Lee et al.*, 2006], yet homopycnal conditions prevail because the small reservoir rapidly becomes turbid itself, blurring the density contrast between inflow and lake. The large Shihmen reservoir, on the other hand, features deposits similar to case D, which become thicker rather than thinner going into the lake. During and after flood, the reservoir is known to host a long-lasting turbid pool at its deep end (S. T. Hsu, Problems encountered in Shihmen reservoir and the improvement plans, paper presented at 1st Taiwan-Japan Workshop on Flood Hazard Mitigation, Hydrotech Research Institute, National Taiwan University, Taipei, Taiwan, 2006), and receives very little coarse sediment load because the latter is intercepted by the Ronghua reservoir. Well-known hyperpycnal deltas having morphologies matching cases B and C are the deltas of the Upper Rhine at Lake Constance [*Hinderer*, 2001], and the Colorado River at Lake Mead [*Graf*, 1971; *Kostic and Parker*, 2003]. The Upper Rhine delta, in a valley of moderate inclination, exhibits a very long topset and a short foreset, whereas the Colorado river delta, in a valley of steeper inclination, features a short topset and an elongated foreset.

6. Conclusion

[12] In this work, we proposed and tested a theory of reservoir infill by delta progradation over bedrock. The theory describes the joint evolution of the river and lake beds under fluvial and hyperpycnal transport, subject to limited sediment supply. Unlike other recent models of deltaic sedimentation [e.g., *Kostic and Parker*, 2003; *Gerber et al.*, 2008], our description is sufficiently simple to be tractable analytically. Nevertheless, it can reproduce the diverse sedimentation patterns generated in experiments. Similar to distributions encountered in actual reservoirs, these patterns include lacustrine deposits of varied curvatures, lengths, and tapers. The theory further predicts, and experiments confirm, that weak sediment supply to the bedrock river can be entirely driven into the lake by hyperpycnal underflows.

[13] **Acknowledgments.** Financial support was provided by the National Science Council and by the Tsung Cho Chang Educational Foundation, Taiwan. F. C. Wu, D. L. Young, L. S. Teng and two anonymous reviewers offered valuable feedback. We also thank M. Larcher and W.-S. Yu for supplying the Froude scale experimental data used to check the scale-independence of our approach.

References

Armanini, A., and M. Larcher (2001), Rational criterion for designing opening of slit-check dam, *J. Hydraul. Eng.*, *127*, 94–104.

Begin, Z. B., D. F. Meyer, and S. A. Schumm (1981), Development of longitudinal profiles of alluvial channels in response to base level lowering, *Earth Surf. Processes Landforms*, *6*, 49–68.

Capart, H., M. Bellal, and D. L. Young (2007), Self-similar evolution of semi-infinite alluvial channels with moving boundaries, *J. Sediment. Res.*, *77*, 13–22.

Dadson, S. J., et al. (2003), Links between erosion, runoff variability and seismicity in the Taiwan orogen, *Nature*, *426*, 648–651.

Fan, J. (1986), Turbid density currents in reservoirs, *Water Int.*, *11*, 107–116.

Gerber, T. P., L. F. Pratson, M. A. Wolinsky, R. Steel, J. Mohr, J. B. Swenson, and C. Paola (2008), Clinoform progradation by turbidity currents: Modeling and experiments, *J. Sediment. Res.*, *78*, 220–238.

Graf, W. H. (1971), *Hydraulics of Sediment Transport*, McGraw-Hill, New York.

Hinderer, M. (2001), Late Quaternary denudation of the Alps, valley and lake fillings and modern river loads, *Geodin. Acta*, *14*, 231–263.

Hsu, J. P. C., and H. Capart (2008), Onset and growth of tributary-dammed lakes, *Water Resour. Res.*, *44*, W11201, doi:10.1029/2008WR007020.

Imaizumi, F., and R. C. Sidle (2007), Linkage of sediment supply and transport processes in Miyagawa Dam catchment, Japan, *J. Geophys. Res.*, *112*, F03012, doi:10.1029/2006JF000495.

Jordan, T. E., and P. B. Flemings (1991), Large-scale stratigraphic architecture, eustatic variation, and unsteady tectonism: A theoretical evaluation, *J. Geophys. Res.*, *96*, 6681–6699.

Kashiwai, J. (2005), Reservoir sedimentation and sediment management in Japan, *Tech. Memo. 3957*, pp. 240–250, Public Works Res. Inst., Tsukuba, Japan.

Kenyon, P. M., and D. L. Turcotte (1985), Morphology of a delta prograding by bulk sediment transport, *Geol. Soc. Am. Bull.*, *96*, 1457–1465.

Kostic, S., and G. Parker (2003), Progradational sand-mud deltas in lakes and reservoirs. Part 1. Theory and numerical modeling, *J. Hydraul. Res.*, *41*, 127–140.

Lai, S. Y. J., and H. Capart (2007), Two-diffusion description of hyperpycnal deltas, *J. Geophys. Res.*, *112*, F03005, doi:10.1029/2006JF000617.

Lee, H.-Y., Y.-T. Lin, and Y.-J. Chiu (2006), Quantitative estimation of reservoir sedimentation from three typhoon events, *J. Hydrol. Eng.*, *11*, 362–370.

Malverti, L., E. Lajeunesse, and F. Métivier (2008), Small is beautiful: Upscaling from microscale laminar to natural turbulent rivers, *J. Geophys. Res.*, *113*, F04004, doi:10.1029/2007JF000974.

Morris, G., and J. Fan (1997), *Reservoir Sedimentation Handbook*, McGraw-Hill, New York.

Muto, T. (2001), Shoreline autoretreat substantiated in flume experiments, *J. Sediment. Res.*, *71*, 246–254.

Swenson, J. B., and T. Muto (2007), Response of coastal plain rivers to falling relative sea-level: Allogenic controls on the aggradational phase, *Sedimentology*, *54*, 207–221.

Toniolo, H., G. Parker, and V. Voller (2007), Role of ponded turbidity currents in reservoir trap efficiency, *J. Hydraul. Eng.*, *133*, 579–595.

Voller, V. R., J. B. Swenson, and C. Paola (2004), An analytical solution for a Stefan problem with variable latent heat, *Int. J. Heat Mass Transfer*, *47*, 5387–5390.

Yu, W.-S., H.-Y. Lee, and S. M. Hsu (2000), Experimental study on delta formation in a reservoir (in Chinese), *J. Chin. Inst. Civ. Hydraul. Eng.*, *12*, 171–177.

H. Capart and S. Y. J. Lai, Department of Civil Engineering and Hydrotech Research Institute, National Taiwan University, Taipei 10617, Taiwan. (hcapart@yahoo.com)